the FEBS Journal

Mechanistic insights into 1-deoxy-D-xylulose 5-phosphate reductoisomerase, a key enzyme of the MEP terpenoid biosynthetic pathway

Heng Li[1], Jie Tian[1], Wei Sun[2], Wei Qin[1] and Wen-Yun Gao[1]

1 Key Laboratory of Resource Biology and Biotechnology in Western China (Ministry of Education), College of Life Sciences, Northwest University, Xi'an, China
2 Key Laboratory of Synthetic and Natural Functional Molecule Chemistry (Ministry of Education), School of Chemistry and Materials Science, Northwest University, Xi'an, China

Keywords
1-deoxy-D-xylulose 5-phosphate; 1-deoxy-D-xylulose 5-phosphate reductoisomerase; binding mode; catalytic cycle; MEP pathway

Correspondence
W.-Y. Gao, Key Laboratory of Resource Biology and Biotechnology in Western China (Ministry of Education), College of Life Sciences, Northwest University, Xi'an, Shaanxi 710069, China
Fax: +86 29 88303572
Tel: +86 29 88303446 ext. 832
E-mail: gaowenyun@nwu.edu.cn

(Received 14 July 2013, revised 2 September 2013, accepted 2 September 2013)

doi:10.1111/febs.12516

The binding mode of 1-deoxy-D-xylulose 5-phosphate (DXP) to 1-deoxy-D-xylulose 5-phosphate reductoisomerase (DXR) (EC 1.1.1.267) from *Escherichia coli* was investigated via ^{18}O isotope exchange experiments and determination of the kinetic parameters of the reaction. The results support a C3–C4 substrate binding mode in which DXP chelates a DXR-bound divalent cation via its hydroxyl groups at C3 and C4. Based on this binding mode and the early results, a catalytic cycle for the conversion of DXP to 2-methyl-D-erythritol 4-phosphate mediated by DXR including a pseudo-single molecule transition state of the retro-aldol intermediates is proposed. Taking into account the binding mode of DXP and the catalytic cycle of DXR, the mechanistic insights of DXR are disclosed and the current discrepancies concerning the catalysis of this enzyme are interpreted within the accepted retro-aldol/aldol sequence.

Introduction

1-Deoxy-D-xylulose 5-phosphate reductoisomerase (DXR), a key enzyme of the recently established 2-methyl-D-erythritol 4-phosphate (MEP) terpenoid biosynthetic pathway, catalyzes the first committed step of this non-mevalonate pathway by converting 1-deoxy-D-xylulose 5-phosphate (DXP) (**1**) to MEP (**2**) in an NADPH- and divalent-metal-dependent manner [1]. Because DXR is a key enzyme of the alternative pathway and also a promising target for new antibiotics, intense research has focused on the elucidation of its catalytic mechanism and the discovery of its inhibitors [2–5]. As a result, the natural metabolite fosmidomycin (**3**), a structural analogue of DXP that was isolated from *Streptomyces lavendulae*, and its congener FR-900098 (**4**) were identified as DXR inhibitors. These compounds had excellent *in vitro* and *in vivo* activities against many bacteria and *Plasmodium* spp. [6–8]. Two mechanisms have been proposed for the DXR-catalyzed reaction (Fig. 1). In the α-ketol rearrangement mechanism (route A), deprotonation of the C-3 hydroxyl group followed by a C4 to C2 alkyl migration yields 2-methyl-D-erythrose 4-phosphate (**5**), which is reduced to **2** by NADPH. In the retro-aldol/aldol mechanism (route B), DXR first cleaves the

Abbreviations
DXP, 1-deoxy-D-xylulose 5-phosphate; DXR, 1-deoxy-D-xylulose 5-phosphate reductoisomerase; MEP, 2-methyl-D-erythritol 4-phosphate.

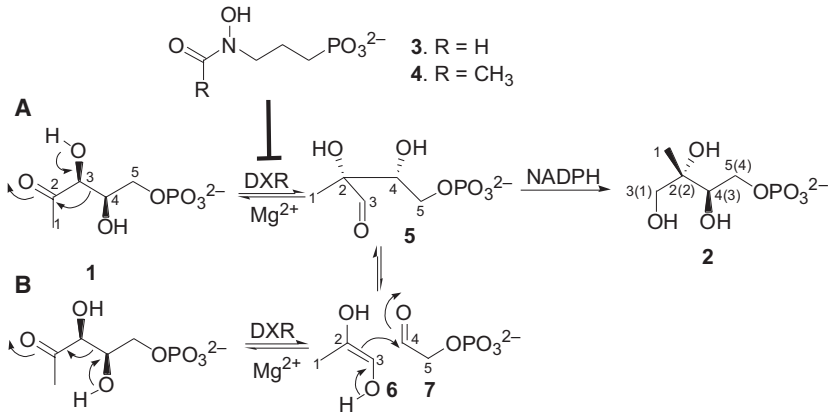

Fig. 1. Two catalytic mechanisms proposed for DXR: route A, α-ketol rearrangement mechanism; route B, retro-aldol/aldol mechanism. The carbons of compounds **2**, **5**, **6** and **7** are numbered in correspondence with those of **1**. For **2**, the digits in parentheses represent the correct numbering.

C3–C4 bond of **1** in a retro-aldol manner to afford two fragments, the enolate of hydroxyacetone **6** and the glycolaldehyde phosphate **7**, which then reunite in an aldol reaction to produce a new C–C bond and generate the same aldehyde intermediate **5** as in route A. The subsequent reduction of **5** by NADPH affords **2**. The accumulated evidence favored the retro-aldol/aldol sequence [9–11]. The mechanism was finally elucidated via determining the kinetic isotope effects by using ^{2}H- or ^{13}C-labeled DXP as substrates [12–14]. The α-ketol rearrangement mechanism was definitively ruled out.

While the retro-aldol/aldol mechanism for DXR has been accepted, some discrepancies have required further investigation. Exogenous **6** and **7**, the two putative intermediates expected from the retro-aldol cleavage, were not recognized by DXR and converted to MEP [11,15,16], even in the presence of high concentrations of **6** (approximately 0.25 M) [15]. In addition, no fragment exchange was detected in the reverse reaction when a mixture of [1-^{13}C]-**2** and [3-^{13}C]-**2** was used as the substrate [15]. These results demonstrated that DXR does not have any aldolase activity and seemed to support the α-ketol mechanism; the explanation for this phenomenon in the context of the retro-aldol/aldol mechanism remains unclear. Meanwhile, it is not known how the substrate DXP binds to DXR. The crystal structure of DXR in complex with the inhibitor fosmidomycin **3** and a divalent metal ion (M^{2+}) has shown that the *N*-formyl hydroxylamine group in **3** provides two oxygen ligands for the M^{2+}, which is present in a distorted octahedral coordination sphere [17–20]. This structure is believed to mimic the substrate binding of the carbonyl oxygen and the C3 hydroxyl group in DXP with the enzyme-bound M^{2+} (C2–C3 binding mode). However, other studies have suggested that the C3 and C4 hydroxyl groups of DXP could be essential for the chelation of M^{2+} (C3–C4 binding mode) [9,16]. Moreover, it has been demonstrated that the reaction intermediates **5**, **6** and **7** remain strictly bound to the enzyme during DXP rearrangement [4,15], but how they bind is yet undetermined.

The oxygen of carbonyl compounds can exchange with solvent $H_2{}^{18}O$ by hydration, and the exchange rate can be accelerated via the addition of acids/bases or by introduction of electron-withdrawing substituents. Normally, ^{18}O exchange occurs slowly with ketones and more rapidly with aldehydes [21]. This phenomenon has been utilized to characterize reaction mechanisms [22–25], detect glycation sites in proteins [26] and accommodate the chemistry of peptides and proteins [27]. In the conversion of DXP **1** to MEP **2**, three carbonyl compounds (substrate **1**, the retro-aldol intermediate **7** and the aldol product **5**) are involved, among which compounds **5** and **7** are aldehydes (Fig. 1). Furthermore, each aldehyde possesses an electron-attracting substituent at its α-position that accelerates the exchange of the carbonyl oxygen with solvent. Therefore, we predict that ^{18}O should be incorporated into MEP through solvent exchange if DXP is incubated with DXR and all the cofactors in an $H_2{}^{18}O$-enriched buffer. Accordingly, we could provide more evidence to deduce the DXP binding mode and could gain mechanistic insights into the DXR-mediated reaction by analyzing the ^{18}O-labeling pattern and enrichment of MEP.

Results

Based on the above prediction, we incubated DXP (20 mg) and *Escherichia coli* DXR (500 μg) in the presence of Mg^{2+} and NADPH in a buffer containing 83% $H_2{}^{18}O$ (500 μL, pH 7.5, 37 °C, 6 h). The product MEP was then analyzed by MS and NMR. Negative mode ESI-MS revealed the existence of unlabeled MEP (*m*/*z* 215, $[M–H]^-$) and MEP with only one ^{18}O

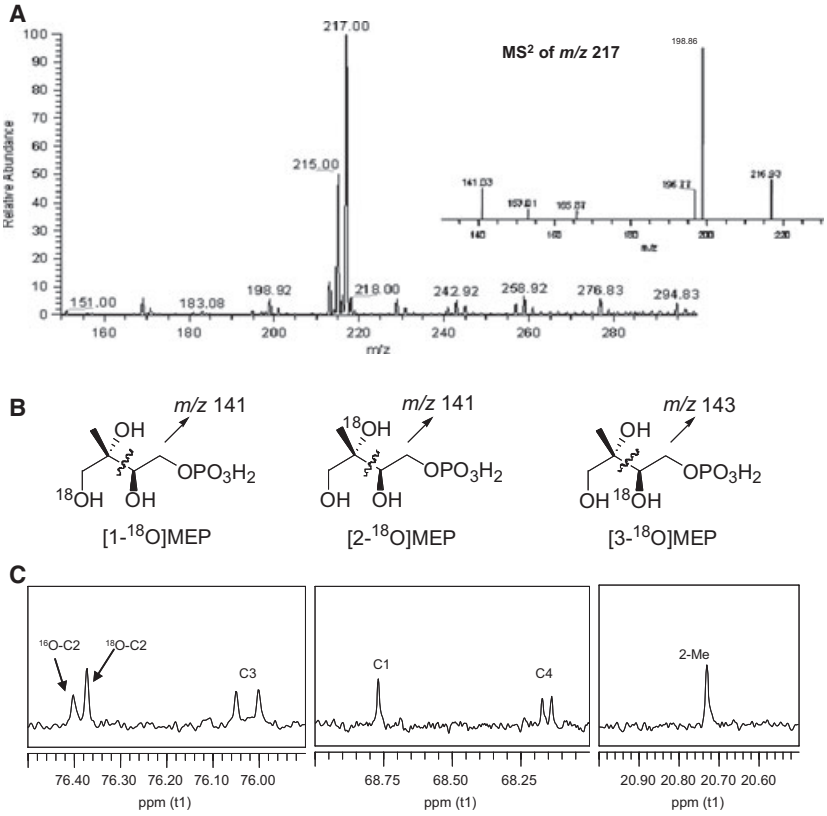

Fig. 2. Negative ESI-MS and ^{13}C-NMR analysis of MEP prepared from unlabeled DXP in an 83% $H_2{}^{18}O$-enriched buffer: (A) negative ESI-MS of MEP (inset: negative ESI-MS^2 of the peak at *m*/*z* 217); (B) analysis of MS fragmentation of single ^{18}O-labeled MEP; (C) ^{13}C-NMR spectrum of MEP.

label (*m*/*z* 217, $[M–H + 2]^-$) in a ratio of approximately 1 : 2 (Fig. 2A). ESI-MS^2 of the peak *m*/*z* 217 produced a peak at *m*/*z* 141 and no peak at *m*/*z* 143 (Fig. 2A, insert), showing that the single ^{18}O-labeled MEP would be [1-^{18}O]MEP or [2-^{18}O]MEP (Fig. 2B). ^{13}C-NMR analysis of the compound (Fig. 2C) demonstrated that the signal at about 76.4 ppm, corresponding to the C2 of MEP [28], was split into two peaks because of the ^{16}O/^{18}O isotope effect on the chemical shift of this carbon [29]. One peak was at 76.403 ppm and the other was at 76.373 ppm (^{18}O-enriched C2, upfield shift 30 ppb). Careful integration of the two singlets indicated that the ratio of ^{16}O-MEP/^{18}O-MEP was also around 1 : 2, which corresponds to the ratio that was determined by MS. The signals of the other four carbons were regular (the reason that the NMR peaks of C3 and C4 appear as doublets is due to the respective coupling of the two carbon atoms with phosphorus [28]). Thus, the existence of [1-^{18}O]MEP was ruled out. These data showed that [2-^{18}O]MEP was generated in the experiment and the ^{18}O content at C2 of MEP that originates from C2 of DXP was high (about 67%), suggesting that the carbonyl group of DXP may not chelate the enzyme-bound M^{2+} and could be freely exchangeable throughout the conversion of DXP to MEP.

The high ^{18}O enrichment at C2 of MEP obtained from the above experiment, however, does not totally eliminate the possibility that the DXP carbonyl group coordinates with M^{2+} because the high ^{18}O content at C2 of DXP could be acquired before DXP binding if the rate of carbonyl exchange with water is much faster than that of the conversion of DXP to MEP, leading to the high ^{18}O incorporation at C2 of MEP. Therefore, we determined the rates of DXP exchange and conversion under conditions that were identical with the previous experiment. To measure the exchange rate of the carbonyl group, DXP (2.0 mg) was incubated in 500 μL of ^{18}O-enriched buffer (83% $H_2{}^{18}O$, 10 mM Mg^{2+}, pH 7.5, 37 °C), and 50-μL aliquots were removed at certain time points and flash-frozen with liquid nitrogen to stop the exchange. After lyophilization, the ^{18}O content at C2 of DXP was determined by ESI-MS and plotted against the exchange time (Fig. 3, curve B). The DXP conversion rate was measured as follows: DXP (0.2 mg) was incubated in 50 μL of ^{18}O-enriched buffer (83% $H_2{}^{18}O$, pH 7.5) containing 50 μg of *E. coli* DXR and all of the necessary cofactors at 37 °C. A 5-μL aliquot was removed, diluted to 500 μL and measured photometrically. The result was plotted as shown in Fig. 3 (curve A). We found that the conversion of DXP was

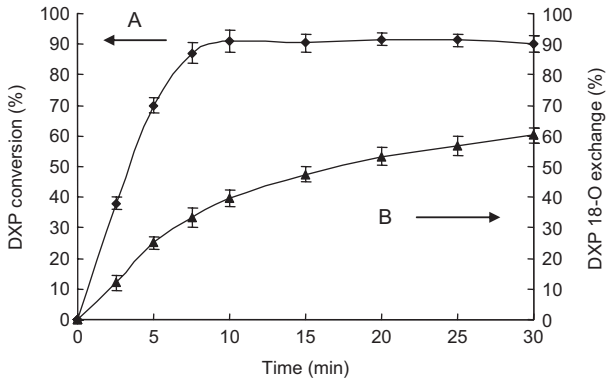

Fig. 3. Comparison of the DXP conversion rate (A) and exchange rate (B).

complete in less than 10 min, while the exchange of the DXP carbonyl group only reached 35% in 10 min. In addition, within this time course, the DXP conversion rate is approximately three times as big as its exchange rate. Based on this experiment, we would deduce that, in the preparation of MEP in ^{18}O-enriched buffer, less than half of the ^{18}O label at C2 was from the exchange that occurred prior to DXP binding, while the other half occurred from the post-binding exchange. Combining the above data, we conclude that the carbonyl group of DXP may not chelate the DXR-bound M^{2+} during the conversion process.

From the MEP preparation experiment we also found that there was no detectable ^{18}O incorporation at either C1 or C3 of MEP. The lack of enrichment at C1 of MEP that originates from C3 of DXP could be due to the fact that in both C2–C3 and C3–C4 binding modes the C3 hydroxy group of DXP chelates the DXR-bound M^{2+} during the conversion process, leading to tight restriction of the retro-aldol intermediate **6** and then the aldol product **5** by chelation, which could completely block the exchange of their carbonyl oxygen atoms with solvent water (Fig. S1). The absence of ^{18}O enrichment at C3 of MEP, however, may not be reasonably explained via the C2–C3 binding mode. Actually, in this binding mode C3 of MEP which originates from C4 of DXP should be labeled by ^{18}O because the C4 hydroxyl group of DXP is not fixed by chelation with the DXR-bound M^{2+}; thus ^{18}O exchange occurs simultaneously upon the formation of the intermediate **7** (although it has been postulated that **7** might be a transient intermediate!) because it has been demonstrated that the compound **7** exists primarily in a hydrated form in aqueous solution [30,31]. But if the C3–C4 binding mode is operative, the phenomenon could be interpreted: the C4 hydroxyl group of DXP was confined by chelation with the DXR-bound M^{2+}, resulting in tight restriction of the retro-aldol intermediate **7**, which could entirely stop the exchange of its carbonyl oxygen atoms (Fig. S1). Thus, it is more likely that C4 of DXP could chelate the DXR-bound M^{2+}.

In order to get further evidence to support that the C4 hydroxy of DXP may coordinate with the M^{2+}, we evaluated the role of the M^{2+} in catalysis by measuring the pH dependence of k_{cat} of the reaction catalyzed by DXR under initial rate conditions with the concentration of NADPH being saturated. The result (Fig. 4) showed that the k_{cat} value is independent of pH in the range $6.2 \leq pH \leq 8.5$, indicating that the DXP conversion mediated by DXR is electrostatic catalysis, not acidic/basic catalysis, because k_{cat} is not expected to alter with pH for such electrostatic catalysis. A similar phenomenon was observed by Argyrou and Blanchard when they worked on *Mycobacterium tuberculosis* DXR [32]. It has been shown that the DXP rearrangement step mediated by the *E. coli* DXR is rate limiting [11]; thus the initial deprotonation of the C4 hydroxy of DXP (the retro-aldol step) should be promoted by electrostatic interaction between the M^{2+} and the OH group. These data favor the above deduction that it could be the C4 hydroxy of DXP that coordinates with the M^{2+} in the retro-aldol step.

Based on all of the above results, we conclude that DXP, the natural substrate of DXR, may bind to DXR via coordination with a DXR-bound divalent cation through a C3–C4 binding mode and not a C2–C3 binding mode.

Given the C3–C4 DXP binding mode and that (a) DXR requires M^{2+} for catalytic activity [1,16,32], (b) DXR follows an ordered mechanism in which

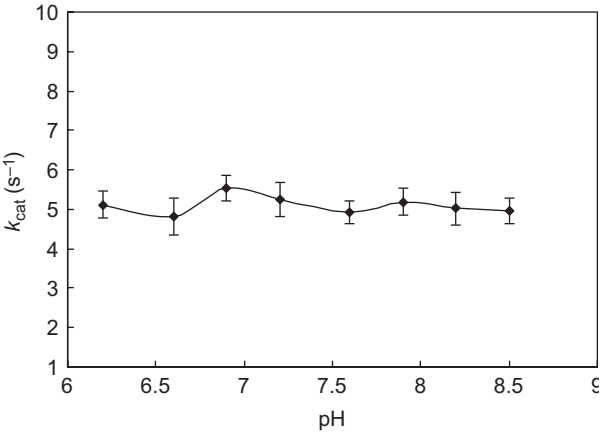

Fig. 4. Determination of the k_{cat} of the reaction catalyzed by DXR at different pH values.

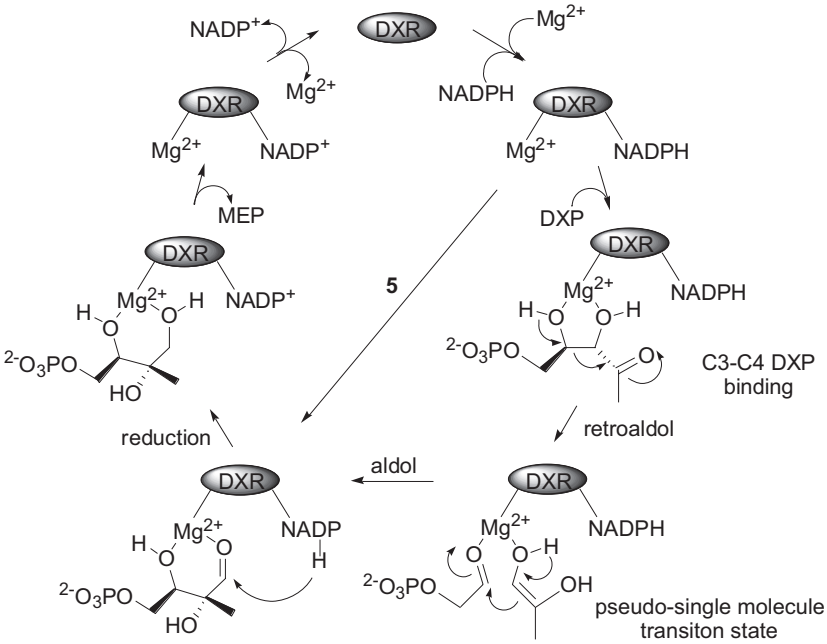

Fig. 5. The proposed DXR catalytic cycle for the conversion of DXP to MEP.

NADPH and M^{2+} bind first preceding the binding of the substrate DXP [16,33], (c) all the reaction segments remain tightly combined to DXR prior to the NADPH reduction [4,15] and (d) after reduction, the final product MEP is released before the discharge of $NADP^+$ [9,16], we propose a catalytic cycle for the rearrangement/reduction reaction mediated by DXR (Fig. 5). First, NADPH and M^{2+} bind to DXR, followed by binding of DXP via coordination of its hydroxyl groups with the DXR-bound M^{2+}. The subsequent deprotonation of the C4 hydroxyl group triggers a retro-aldol cleavage of the C3–C4 bond of DXP, generating the two intermediates **6** and **7** which remain tightly coordinated to the metal ion. These intermediates are then recombined in an aldol reaction, affording the aldehyde phosphate **5** in which the carbonyl O atom and 3-hydroxyl group chelate the M^{2+}. The reduction of **5** by hydride addition from the pro-*S* C-4 of NADPH to the *Re* face of the aldehyde results in the formation of the final product with the correct stereochemistry [32,34–36]. The subsequent release of MEP and further discharge of $NADP^+$ and M^{2+} terminate the catalytic cycle. The reverse reaction sequence would take place in the opposite direction, although the equilibrium largely favors the formation of MEP [15,16].

Discussion

The MEP pathway is a recently established route for terpenoid biosynthesis that is operative in most human pathogens but not in humans, and all of the enzymes of the pathway are considered good targets for the screening of antibiotics. One of the most promising targets, DXR, catalyzes the conversion of DXP to MEP through a divalent-cation- and NADPH-dependent isomerization and reduction. The natural compounds fosmidomycin **3**, its congener FR900098 **4** and tens of synthetic analogues have been characterized as efficient inhibitors of DXR. Unfortunately, none of these compounds is currently in clinical use [2]. Two catalytic mechanisms for DXR have been proposed, and the retro-aldol/aldol mechanism has been accepted.

Three-dimensional structures of DXR from different sources in complex with cofactors have revealed the binding mode of **3** [17–20]. Because DXP can be superimposed onto the inhibitor, the C2–C3 binding mode of DXP was accepted and used to explain the enzymatic reaction (Fig. 6) [4,5,17–19]. Deprotonation of the C-4 hydroxyl group of DXP leads to cleavage of the C3–C4 bond and generation of the enolate of hydroxyacetone **6**, which is stabilized by coordination with M^{2+}, and the glycolaldehyde phosphate **7**, which is free from chelation. The subsequent recombination of **6** and **7** via an aldol reaction results in the formation of a C–C bond between carbon atoms C2 and C4 (of DXP) and produces the intermediate 2-methyl-D-erythrose 4-phosphate **5**. Reduction of **5** by NADPH yields the product MEP.

Although the crystal structures of DXR complexed with M^{2+} and **3** have provided insights into the architecture of the active site, the binding format of **3** may

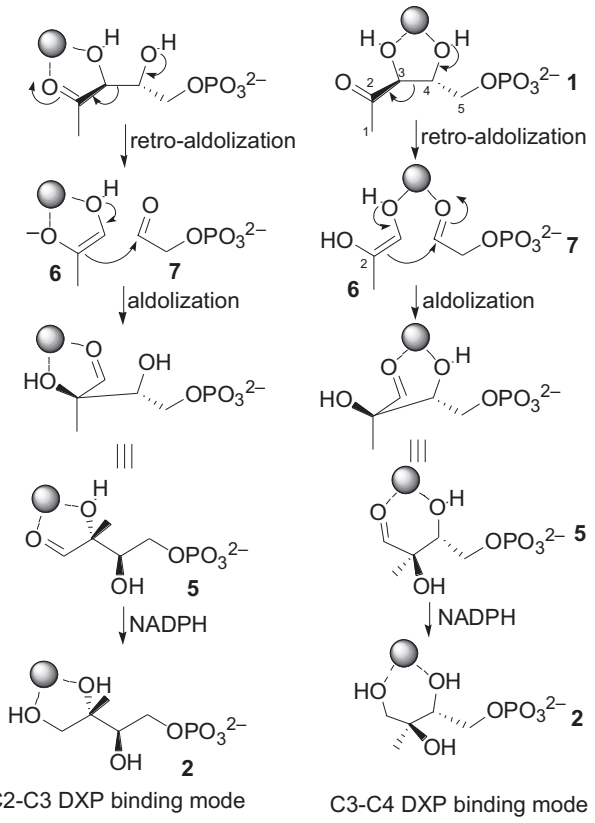

Fig. 6. The conversion of DXP to MEP in the two different DXP binding modes.

not accurately represent the C2–C3 binding mode of DXP because the crystals of the DXR–M^{2+}–**3** complexes were prepared under mildly acidic conditions (pH 5.0–5.8) that differ from the functional pH of the enzyme [17–20]. Therefore, the protonation state of the clustered acidic residues in the active site may be different from that in the active enzyme [5]. Weakly acidic conditions decrease the affinity of the M^{2+} for DXR and block the formation of the octahedral geometry of the active site residues, which is essential for M^{2+} binding [17,18]. In addition, the C2–C3 substrate binding mode does not properly explain the conversion process. (a) The retro-aldol step is initiated by the deprotonation of the C4 hydroxyl group. It has been demonstrated by this study and Argyrou and Blanchard [32] that this process is assisted by electrostatic interaction between the M^{2+} and the OH group (Fig. 6). But in the C2–C3 substrate binding mode, there is no electrostatic force between the C4 hydroxy and the M^{2+} because the C4 OH does not coordinate with M^{2+}. (b) The retro-aldol product **6** might be stabilized by bidentate chelation with M^{2+}, but its nucleophilicity could be reduced because of the electrostatic interaction. Compound **7** is not coordinated with M^{2+}, so its carbonyl group is unactivated. These two factors could increase the barrier of the subsequent aldol reaction. (c) The tentatively bound state of aldehyde **7** contradicts the reported results [4,15] and what we have observed in this study. If **7** is not tightly bound, ^{18}O isotope exchange would occur at its carbonyl group because **7** primarily exists in a hydrated form in aqueous medium [30,31]. (d) In this binding mode, extraneous **6** and **7** should be converted by DXR because they would bind respectively to the enzyme and then recombine to give the aldol intermediate **5**. This deduction is also in opposition to the published data that showed that DXR has not exhibited any aldolase activity [11,15,16].

Early studies have demonstrated that the hydroxyl groups of DXP are essential for rearrangement during the conversion of DXP to MEP because they act as Lewis acids to facilitate the reaction and are probably the sites for divalent cation chelation [9,16,37]. Our observations support this binding mode of DXP. Considering the C3–C4 DXP binding model, the conversion of DXP to MEP could be interpreted as follows (Fig. 6). (a) The coordination of the hydroxyl groups of DXP with M^{2+} increases their acidity and therefore facilitates deprotonation of the C4 hydroxy, which could be fundamental for the retro-aldol reaction. (b) The intermediates **6** and **7** both coordinate with M^{2+} as monodentate ligands and could be strictly constrained [4,15]. (c) Although the enolate **6** is only partially stabilized in this binding mode, its C2 could be a better nucleophile because it has more carbanionic character [38] than it would as a bidentate ligand in the C2–C3 binding mode. In addition, **7** would be polarized upon chelation with M^{2+} through formation of a partial positive charge on the carbonyl C atom, which would enhance its electrophilicity. More importantly, the respective coordination of these two fragments with M^{2+} could create a pseudo-single molecule and thus make the aldol reaction pseudo-intramolecular. These positive aspects could largely benefit the aldol reaction. (d) The restricted state of intermediate **7** would completely inhibit the hydration of its carbonyl group, and therefore the introduction of ^{18}O at this position was not observed in the conversion of DXP to MEP. (e) The coordination of **5** with M^{2+} via its carbonyl and C3 hydroxy could not only induce a partial positive charge on the carbonyl group, enhancing hydride transfer from NADPH, but orient the intermediate as well. Additionally, this coordination also blocks the hydration of the carbonyl group, preventing ^{18}O isotope exchange.

Based on the C3–C4 DXP binding mode and the model of the DXR catalytic cycle, the details of the

DXR mechanism could be interpreted in terms of a retro-aldol/aldol reaction sequence. Exogenous retro-aldol intermediates **6** and **7** cannot be reunited by aldolization to form **5** [11,15,16] because the two fragments and the DXR-bound M^{2+} actually constitute a termolecular reaction system in which the simultaneous coordination of **6** and **7** with M^{2+} to form a pseudo-single molecule would be infrequent. The fragments are not exchanged between the different substrate molecules [15] because aldolization occurs in a pseudo-intramolecular reaction. This pseudo-intramolecular reaction may also explain why DXR does not exhibit any aldolase activity. The intermediacy of **5** is accepted because DXR can convert externally added **5** to MEP in the presence of NADPH or DXP in the presence of $NADP^+$ [16]. However, the existence of **5** has never been determined directly or indirectly, and it is postulated to be a transient intermediate that is not released from the enzyme during catalysis [1,16,34,39]. Our data support this hypothesis: in the catalytic cycle, **5** is strictly restrained by coordination with the DXR-bound metal ion until it is reduced by NADPH to the final product MEP. DXR probably recognizes exogenous **5** because the intact molecule could readily chelate M^{2+} and form the active complex of the catalytic cycle (Fig. 5).

Conclusions

The ^{18}O isotope exchange experiments and k_{cat} determination conducted in this study provide many insights into the DXR-catalyzed rearrangement/reduction of DXP **1** to MEP **2**. The observations support a C3–C4 DXP binding mode which was postulated in previous studies. In conjunction of this DXP binding mode with the early results, a catalytic cycle for DXR including a pseudo-single molecule transition state of the retro-aldol intermediates is proposed through which the current discrepancies in the investigations of the DXR mechanism can be explained in the context of the accepted retro-aldol/aldol sequence. Furthermore, the tight restriction manner of the reaction intermediates by DXR-bound M^{2+} in the conversion process can also be described. This detailed mechanistic information will facilitate the rational design of specific DXR inhibitors that hold promise for the development of new antibacterial and antimalarial agents.

Materials and methods

The plasmid pET15b-DXR, which encodes the *E. coli* gene for recombinant DXR, was a kind gift from C. Dale Poulter of the Chemistry Department at the University of Utah. The bacterial strain *E. coli* BL21(DE3) was obtained from a stock maintained by this institute (College of Life Sciences, Northwest University). The other materials used were as follows: Ni^{2+}-nitrilotriacetic acid agarose resin was purchased from Qiagen (Hilden, Germany); NADPH and sodium pyruvate were purchased from Fluka (http://www.fluka.org); $H_2{}^{18}O$ (97 at% ^{18}O) was the product of the Shanghai Engineering Research Center for Stable Isotopes (Shanghai, China). DXP was synthesized according to procedures previously published by this laboratory [40]. All other chemicals used were of analytical reagent grade. ^{13}C-NMR spectra were collected on a Varian Inova-600 MHz NMR spectrometer. ESI-MS was performed with a Thermo Fisher LTQ XL system.

Preparation of recombinant *E. coli* DXR

The expression and purification of *E. coli* DXR were performed according to the reported method [33]. The plasmid pET15b-DXR was transformed into *E. coli* BL21(DE3) competent cells. LB-ampicillin cultures (3 mL) were inoculated with single colonies, grown overnight at 37 °C and used to inoculate 500 mL LB-ampicillin. The cultures were grown at 37 °C to an D_{600} of 0.4–0.6, the temperature was lowered to 30 °C, isopropyl thio-β-D-galactoside was added to a final concentration of 2 mM, and the incubation was continued for 8 h. The cells were harvested by centrifugation (6300 ***g***). The protein was purified by metal-affinity chromatography on Ni-nitrilotriacetic acid agarose according to the manufacturer's protocol. The protein samples were analyzed by SDS/PAGE and stained with Coomassie Blue R. The purified protein was resuspended in 5–8 mL of 20 mM Tris/HCl buffer (pH 8.0) and dialyzed twice against the same buffer. A final dialysis was performed against 20 mM Tris/HCl buffer (pH 8.0) containing 5 mM dithiothreitol and 20% glycerol. The protein samples were aliquoted into 0.5-mL Eppendorf tubes (50 μL each), flash-frozen and stored at −80 °C. Protein concentrations were determined by the Bradford method using BSA as a standard; the yield of purified protein was 16 $mg \cdot L^{-1}$. The enzymes used in this study retained the His6-tag for purification.

Formation of [2-^{18}O]MEP from unlabeled DXP in an $H_2{}^{18}O$-enriched buffer

The reaction mixture contained 120 mM Tris/HCl (pH 7.5), 20 mg of unlabeled DXP (0.093 mmol), 86 mg of NADPH (0.1 mmol), 10 mM $MgCl_2$, 2 mM dithiothreitol and 500 μg of recombinant *E. coli* DXR in a total volume of 500 μL ($H_2{}^{18}O$% = 83%). After incubation at 37 °C for 6 h, the assay was terminated by heating in boiling water for 3 min. The product was purified following a protocol similar to that for the purification of DXP [40]. After isolation on a DEAE Sephadex A-25 column at 4 °C, the fractions containing MEP were pooled, evaporated to a small volume *in vacuo* and lyophilized. MEP was obtained as the

ammonium salt as a white powder (14.7 mg, yield 72%), and the identity of the product was confirmed by ESI-MS and ^{13}C-NMR. ESI-MS (negative mode) *m*/*z* (%): 215 [M–H]$^-$ (33.7%), 217 [M–H + 2]$^-$ (66.3%). ^{13}C-NMR (150 MHz, D_2O): 76.403 (s, ^{16}O–C-2, 35.3%), 76.373 (s, ^{18}O–C-2, 64.7%), 76.025 (d, *J* 7.4, C-3), 68.770 (s, C-1), 68.155 (d, *J* 5.1, C-4), 20.730 (s, 2-Me).

Determination of the rate of DXR-catalyzed conversion of DXP to MEP

A reaction mixture containing 120 mM Tris/HCl (pH 7.5), 0.2 mg of unlabeled DXP (0.93 μmol), 0.86 mg of NADPH (1.0 μmol), 10 mM $MgCl_2$, 2 mM dithiothreitol and 50 μg of DXR in a final volume of 50 μL ($H_2{}^{18}O$% = 83%) was incubated at 37 °C. At certain time intervals (2.5, 5.0, 7.5, 10 min etc.), a 5-μL aliquot was removed and diluted with double-distilled H_2O to 500 μL, and the UV absorbance was measured at 340 nm. The DXP conversion was then plotted against the reaction time.

Determination of the exchange rate of DXP carbonyl group

An exchange mixture containing 120 mM Tris/HCl (pH 7.5), 10 mM Mg^{2+} and 2 mg of unlabeled DXP in a final volume of 500 μL ($H_2{}^{18}O$% = 83%) was incubated at 37 °C. At certain time intervals (2.5, 5.0, 7.5, 10 min etc.), a 50-μL aliquot was removed, flash-frozen with liquid nitrogen to stop exchange and lyophilized. After re-dissolving in 50 μL methanol (HPLC grade, water content less than 0.03%), the ^{18}O content of DXP was determined immediately by ESI-MS and plotted against the exchange time.

Determination of the k_{cat} of the reaction catalyzed by DXR at different pH values

To determine the k_{cat} of the reaction catalyzed by DXR at different pH values, assays were carried out in a 50 mM Na_2HPO_4-KH_2PO_4 buffer (pH 6.0–7.0) or 100 mM Tris/HCl buffer (pH 7.0–9.0) containing 3 mM $MgCl_2$, 2 mM β-mercaptoethanol and 0.36 mM NADPH at 37 °C. The concentration of DXP varied from 30 to 360 μM. The reactions were initiated by addition of DXR (84 nM) and followed by monitoring the consumption of NADPH at 340 nm. The K_m and V_{max} were obtained by fitting the data to the Michaelis–Menten equation using GRAPHPAD PRISM and k_{cat} was calculated from V_{max}. Typically, initial rates were measured for 2–10% consumption of NADPH.

Acknowledgements

This work was supported by the National Science Foundation of China (NSFC, 21172179), the Program for Changjiang Scholars and Innovative Research Team in University (No. IRT1174), the PhD program of the Ministry of Education of China (20116101110001), and the Northwest University scientific funds (12NW17) and innovation funds for graduate students (10YYB02). We gratefully acknowledge Professor C. Dale Poulter, Chemistry Department, University of Utah, for providing the plasmid pET15b-DXR. We also thank Professor Z. F. Wang and Dr C. N. Xiao of the Institute of Northwest University for respective assistance with the ESI-MS measurements and ^{13}C-NMR determination.

References

1 Takahashi S, Kuzuyama T, Watanabe H & Seto H (1998) A 1-deoxy-D-xylulose 5-phosphate reductoisomerase catalyzing the formation of 2-C-methyl-D-erythritol 4-phosphate in an alternative nonmevalonate pathway for terpenoid biosynthesis. *Proc Natl Acad Sci USA* **95**, 9879–9884.

2 Rohmer M (2010) Methylerythritol phosphate pathway. In Comprehensive Natural Products II, Chemistry and Biology (Mander L & Liu HW, eds), Vol. 1, pp. 517–555. Elsevier, New York.

3 Kuntz L, Tritsch D, Grosdemange-Billiard C, Hemmerlin A, Willem A, Bach TJ & Rohmer M (2005) Isoprenoid biosynthesis as a target for antibacterial and antiparasitic drugs: phosphonohydroxamic acids as inhibitors of deoxyxylulose phosphate reductoisomerase. *Biochem J* **386**, 127–135.

4 Singh N, Chevé G, Avery MA & McCurdy CR (2007) Targeting the methylerythritol phosphate (MEP) pathway for novel antimalarial, antibacterial and herbicidal drug discovery: inhibition of 1-deoxy-D-xylulose-5-phosphate reductoisomerase (DXR) enzyme. *Curr Pharm Design* **13**, 1161–1177.

5 Proteau PJ (2004) 1-Deoxy-D-xylulose 5-phosphate reductoisomerase: an overview. *Bioorg Chem* **32**, 483–493.

6 Jomaa H, Wiesner J, Sanderbrand S, Altincicek B, Weidemeyer C, Hintz M, Türbachova I, Eberl M, Zeidler J, Lichtenthaler HK *et al.* (1999) Inhibitors of the nonmevalonate pathway of isoprenoid biosynthesis as antimalarial drugs. *Science* **285**, 1573–1576.

7 Fernandes RPM, Phaosiri C & Proteau PJ (2005) Mutation in the flexible loop of 1-deoxy-D-xylulose 5-phosphate reductoisomerase broadens substrate utilization. *Arch Biochem* **444**, 159–164.

8 Missinou MA, Borrmann S, Schindler A, Issifou S, Adegnika AA & Matsiegui PB (2002) Fosmidomycin for malaria. *Lancet* **360**, 1941–1942.

9 Wong A, Munos JW, Devasthali V, Johnson KA & Liu HW (2004) Study of 1-deoxy-D-xylulose-5-phosphate reductoisomerase: synthesis and evaluation

of fluorinated substrate analogues. *Org Lett* **6**, 3625–3628.
10 Fox DT & Poulter CD (2005) Synthesis and evaluation of 1-deoxy-D-xylulose 5-phosphoric acid analogues as alternate substrates for methylerythritol phosphate synthase. *J Org Chem* **70**, 1978–1985.
11 Fox DT & Poulter CD (2005) Mechanistic studies with 2-methyl-D-erythritol 4-phosphate synthase from *Escherichia coli*. *Biochemistry* **44**, 8360–8368.
12 Wong U & Cox RJ (2007) The chemical mechanism of D-1-deoxyxylulose-5-phosphate reductoisomerase from *Escherichia coli*. *Angew Chem Int Ed* **46**, 4926–4929.
13 Munos JW, Pu X, Mansoorabadi SO, Kim HJ & Liu HW (2009) A secondary kinetic isotope effect study of the 1-deoxy-D-xylulose-5-phosphate reductoisomerase-catalyzed reaction: evidence for a retroaldol-aldol rearrangement. *J Am Chem Soc* **131**, 2048–2049.
14 Manning KA, Sathyamoorthy B, Eletsky A, Szyperski T & Murkin AS (2012) Highly precise measurement of kinetic isotope effects using 1H-detected 2D [13C,1H]-HSQC NMR spectroscopy. *J Am Chem Soc* **134**, 20589–20592.
15 Lauw S, Illarionova V, Bacher A, Rohdich F & Eisenreich W (2008) Biosynthesis of isoprenoids – studies on the mechanism of 2C-methyl-D-erythritol-4-phosphate synthase. *FEBS J* **275**, 4060–4073.
16 Hoeffler JF, Tritsch D, Grosdemange-Billiard C & Rohmer M (2002) Isoprenoid biosynthesis via the methylerythritol phosphate pathway. Mechanistic investigations of the 1-deoxy-D-xylulose 5-phosphate reductoisomerase. *Eur J Biochem* **269**, 4446–4457.
17 Steinbacher S, Kaiser J, Eisenreich W, Huber R, Bacher A & Rohdich F (2003) Structural basis of fosmidomycin action revealed by the complex with 2-C-methyl-D-erythritol 4-phosphate synthase (IspC). *J Biol Chem* **278**, 18401–18407.
18 Sweeney AM, Lange R, Fernandes RPM, Schulz H, Dale GE, Douangamath A, Proteau PJ & Oefner C (2005) The crystal structure of *E coli* 1-deoxy-D-xylulose-5- phosphate reductoisomerase in a ternary complex with the antimalarial compound fosmidomycin and NADPH reveals a tight-binding closed enzyme conformation. *J Mol Biol* **345**, 115–127.
19 Henriksson LM, Unge T, Carlsson J, Åqvist J, Mowbray SL & Jones TA (2007) Structures of *Mycobacterium tuberculosis* 1-deoxy-D-xylulose-5-phosphate reductoisomerase provide new insights into catalysis. *J Biol Chem* **282**, 19905–19916.
20 Yajima S, Hara K, Iino D, Sasaki Y, Kuzuyama T, Ohsawa K & Seto H (2007) Structure of 1-deoxy-D-xylulose 5-phosphate reductoisomerase in a quaternary complex with a magnesium ion, NADPH and the antimalarial drug fosmidomycin. *Acta Cryst* **F63**, 466–470.
21 Bell RP (1966) The reversible hydration of carbonyl compounds. *Advanc Phys Org Chem* **4**, 1–29.
22 Wilgis FP, Neumann TE & Shiner VJ Jr (1990) Mechanism of solvolysis of 1-(1-adamantyl)ethyl sulfonates. *J Am Chem Soc* **112**, 4435–4446.
23 Grée D, Grée R, Lowinger TB, Martelli J, Negri JT & Paquette LA (1992) Acid-catalyzed cyclization of 1,4-diols tethered to (butadiene)iron tricarbonyl segments. Isotopic labeling as a mechanistic probe of stereochemical retention during tetrahydrofuran formation. *J Am Chem Soc* **114**, 8841–8846.
24 Cane DE, Du S & Spenser ID (2000) Biosynthesis of vitamin B6: origin of the oxygen atoms of pyridoxol phosphate. *J Am Chem Soc* **122**, 4213–4214.
25 Chau ST, Hayakawa Y & Sulikowski GA (2011) 18O Assisted analysis of a γ, δ-epoxyketone cyclization: synthesis of the C16–C28 fragment of ammocidin D. *Org Lett* **13**, 756–759.
26 Kijewska M, Stefanowicz P, Kluczyk A & Szewczuk Z (2011) The isotopic exchange of oxygen as a tool for detection of the glycation sites in proteins. *Anal Biochem* **419**, 81–87.
27 Fernandez-de-Cossio J (2011) Mass spectrum patterns of ^{18}O-tagged peptides labeled by enzyme-catalyzed oxygen exchange. *Anal Chem* **83**, 2890–2896.
28 Hoeffler JF, Pale-Grosdemange C & Rohmer M (2000) Chemical synthesis of enantiopure 2-C-methyl-D-erythritol 4-phosphate, the key intermediate in the mevalonate-independent pathway for isoprenoid biosynthesis. *Tetrahedron* **56**, 1485–1489.
29 Risley JM & Van Etten RL (1979) An oxygen-18 isotope shift upon carbon-13 NMR spectra and its application to the study of oxygen exchange kinetics. *J Am Chem Soc* **101**, 252–253; **102**, 4609–4614; **102**, 6699–6702.
30 Müller D, Pitsch S, Kittaka A, Wagner E, Wintner CE & Eschenmoser A (1990) Chemistry of α-aminonitriles. Aldomerization of glycolaldehyde phosphate to *rac*-hexose 2,4,6-triphosphates and *rac*-pentose 2,4-diphosphates: *rac*-allose 2,4,6-triphosphate and *rac*-ribose 2,4-diphosphate are the main reaction products. *Helv Chim Acta* **73**, 1410–1468.
31 Johnson AE & Tanner ME (1998) Epimerization via carbon-carbon bond cleavage. L-Ribulose-5-phosphate 4-epimerase as a masked class II aldolase. *Biochemistry* **37**, 5746–5754.
32 Argyrou A & Blanchard JS (2004) Kinetic and chemical mechanism of *Mycobacterium tuberculosis* 1-deoxy-D-xylulose-5-phosphate isomeroreductase. *Biochemistry* **43**, 4375–4384.
33 Koppisch AT, Fox DT, Blagg BSJ & Poulter CD (2002) *E coli* MEP synthase: steady-state kinetic analysis and substrate binding. *Biochemistry* **41**, 236–243.
34 Proteau PJ, Woo YH, Williamson RT & Phaosiri C (1999) Stereochemistry of the reduction step mediated

by recombinant 1-deoxy-D-xylulose 5-phosphate isomeroreductase. *Org Lett* **1**, 921–923.
35 Radykewicz T, Rohdich F, Wungsintaweekul J, Herz S, Kis K, Eisenreich W, Bacher A, Zenk MH & Arigoni D (2000) Biosynthesis of terpenoids: 1-deoxy-D-xylulose-5-phosphate reductoisomerase from *Escherichia coli* is a class B dehydrogenase. *FEBS Lett* **465**, 157–160.
36 Arigoni D, Giner JL, Sagner S, Wungsintaweekul J, Zenk MH, Kis K, Bacher A & Eisenreich W (1999) Stereochemical course of the reduction step in the formation of 2C-methylerythritol from the terpene precursor 1-deoxyxylulose in higher plants. *Chem Commun* **1999**, 1127–1128.
37 Phaosiri C & Proteau PJ (2004) Substrate analogs for the investigation of deoxyxylulose 5-phosphate reductoisomerase inhibition: synthesis and evaluation. *Bioorg Med Chem Lett* **14**, 5309–5312.
38 Deupree JD & Wood WA (1972) L-Ribulose-5-phosphate 4-epimerase from *Aerobacter aerogenes*: evidence for a role of divalent metal ions in the epimerization reaction. *J Biol Chem* **247**, 3093–3097.
39 Rohmer M, Seemann M, Horbach S, Bringer-Meyer S & Sahm H (1996) Glyceraldehyde 3-phosphate and pyruvate as precursors of isoprenic units in an alternative non-mevalonate pathway for terpenoid biosynthesis. *J Am Chem Soc* **118**, 2564–2566.
40 Li H, Tian J, Wang H, Yang SQ & Gao WY (2010) An improved preparation of D-glyceraldehyde 3-phosphate and its use in the synthesis of 1-deoxy-D-xylulose 5-phosphate. *Helv Chim Acta* **93**, 1745–1750.

Supporting information

Additional supporting information may be found in the online version of this article at the publisher's web site:

Fig. S1. Possible ^{18}O-labeling pattern of MEP prepared from unlabeled DXP in an $H_2{}^{18}O$-containing buffer: (A) under C2–C3 DXP binding mode; (B) under C3–C4 DXP binding mode.